Document ID
1983850, (1.0 Approved)
Reg no

Security class
Public

Page
1(13)

Document type
Report

Author
2022-06-10 Mattias Åkesson
Heikki Laitinen

Quality assurance
2022-08-19 Mattias Åkesson (RR)
2022-08-29 Lotta Rubio Lind (Approved)

Gas phase composition during the unsaturated period. Status report June 2022.

Contents

1 Introduction

The overall objective of this work is to investigate the evolution of gases in unsaturated bentonites. The consumption of O_2 and the production of H_2S are of particular interest. Investigations of the evolution of gases under such conditions have previously been reported by Birgersson and Goudarzi (2018). Åkesson et al. (2020) presented results from the initial tests performed with an equipment in which the bentonite was subjected to a thermal gradient provided by a centrally placed heater, made of either copper or stainless steel. The results from these latter tests indicated that the rate of oxygen consumption was approximately the same in the two tests, regardless if the heater was made of copper or of stainless steel, and this suggested that the oxygen consumption was caused by processes in the bentonite rather than by oxidation of the metal, which is in direct conflict to the conclusions in Birgersson and Goudarzi (2018). This equipment was subsequently modified in different ways:

i. By developing a new test setup in which the bentonite can be placed inside a gastight glass container, which in turn is placed in a temperature chamber. This means that the gas composition evolution can be investigated in the absence of any metals and with isothermal conditions.
ii. By installation of condensation traps, which can prevent the hot vapour from entering the gas analysis system.
iii. By expanding the measuring ranges for some of the gas sensors, especially for the H_2-sensor which was found to be too narrow in the initial tests.
iv. By using a bentonite with a higher content of sulphur. This will the enhance the prospects of quantifying gases formed as a result of oxidation or dissolution of pyrite.

A new test programme, described in the activity plan AP RD LERMTRL-20-018, was launched in the beginning of 2021. This status report presents the main results obtained within the framework of this activity plan during the first 18 months of measurements.

2 Materials and methods

2.1 Test equipment

Two sets of test equipment have been used in this work: i) a setup with a *thermal gradient* and a copper heater surrounded by bentonite, which in turn was installed in a stainless-steel container, and ii) the new *isothermal* setup with a glass container in a heating cabinet. The first set (***Figure 2-1***) was identical the one used for the initial tests (see Åkesson et al. 2020) apart from the actual heating mechanism, which was changed from a system with circulating oil to an electrical heating coil installed inside the copper heater, and the construction of a perforated cage which can be placed on top of the heater which means that fairly fine-grained bentonite material can be installed directly (thereby avoiding any block compaction). The second set consisted of a two-parted glass desiccator with a two-hole rubber stopper in the upper part, through which two gas sampling glass tubes were connected and led down into the container (***Figure 2-2***). Each set was connected to a condensation trap; with the copper heater setup the condensate can be led back to the container, whereas for the glass container setup the condensate has to be collected. The entire test system with test setups, condensation traps and the gas analysis system, connected with a number of valves, is illustrated in ***Figure 2-3***.

The gas analysis system was supplied by OmniProcess AB and was designed to measure the concentration of the following gases: oxygen (O_2), carbon dioxide (CO_2), hydrogen (H_2), hydrogen sulphide (H_2S) and sulphur dioxide (SO_2). A compilation of manufacturers, names, methods, measuring intervals and required flow rates is shown in Table 2-1. The original measuring range of the H_2-sensor was 0 -150 ppm. This has subsequently been expanded to 0 – 1000 ppm. The

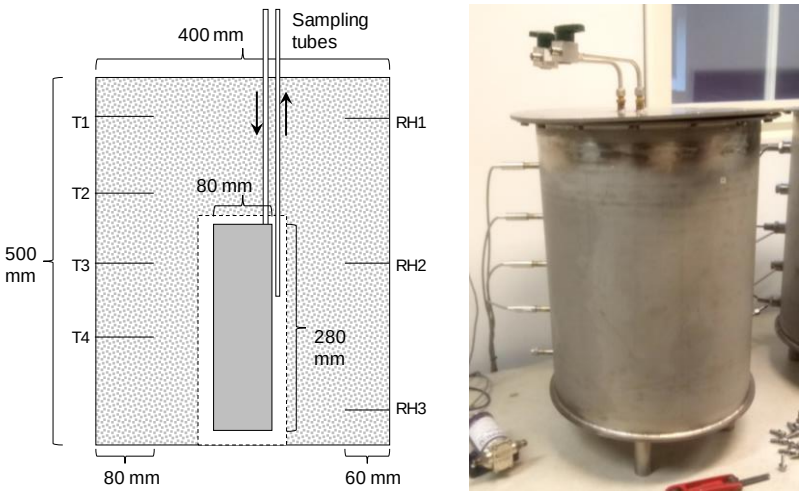

***Figure 2-1**. Test container with copper heater. Schematic section drawing with marked location of temperature and relative humidity sensors (left).*

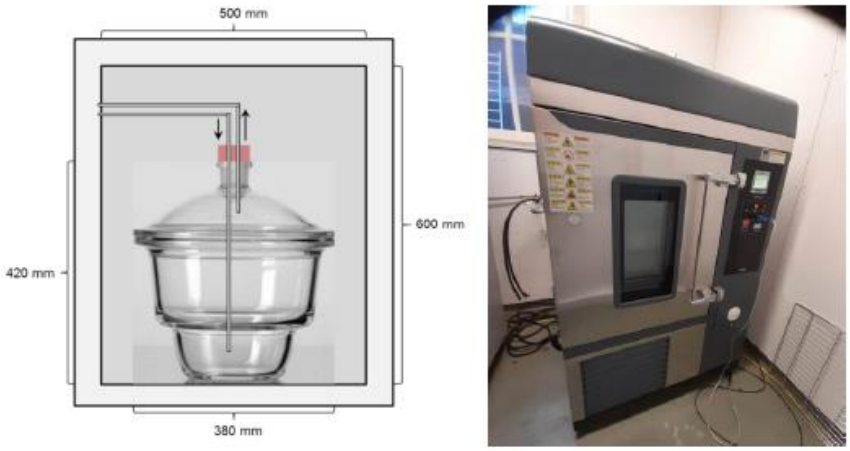

***Figure 2-2**. Glass container (left) in heating cabinet (right).*

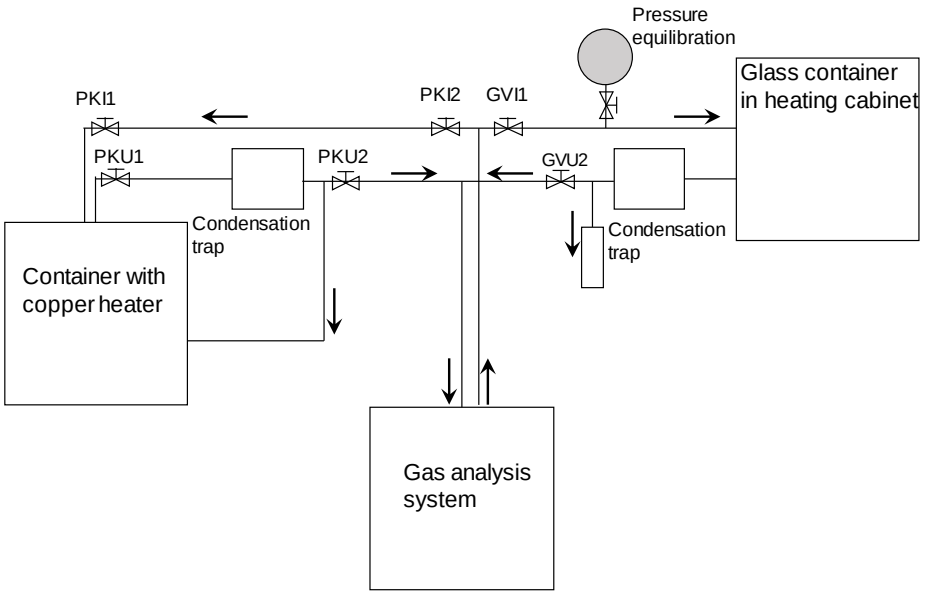

***Figure** 2-3**. Schematic flow scheme over test equipment and gas analysis system.*

measuring range of the CO_2 sensor was also expanded during the preparation for this work; from 0 – 1000 ppm to 0 – 20 %.

Sensor validation
Calibration gases were procured in order to obtain an independent validation of the different sensors. Three gas mixtures in separate tubes were obtained from Air Liquide Gas AB:

- CO_2 (10%) and H_2 (500 ppm) mixed in N_2
- H_2S (5 ppm) mixed in N_2
- SO_2 (0.5 ppm) mixed in N_2

All of these gases could be used through the calibration inlet of the gas analysis system so that the pump determines the flow rate through the different sensors. However, due to the pump in the SO_2-sensor, this had to be tested separately (see ***Figure*** 2-4). No special gas was obtained for O_2, since a well-defined concentration is provided by air. The results from these tests are compiled in Table 2-2. It can be noted that the results for the CO_2, H_2S and SO_2 sensors are in fairly well agreement with, and are generally within 10 %, from the concentration of the calibration gases. The results from the H_2-sensor suggest that the measured concentration underestimates the actual concentration with a factor of 2. The data from this sensor should therefore be regarded as quite uncertain.

Table 2-1. **Compilation of instruments and their characteristics**

Gas	Manufacturer	Instrument	Method	Measuring interval	Flow rate (l/min)
O_2	Servomex	Multiexact 4100	Paramagnetic cell	0 – 25 %	0.1
CO_2	Vaisala	GMP343	NDIR infrared cell	0 – 20 %	0.1
H_2	Compur	Statox 501	Electrochemical cell	0 – 1000 ppm	0.1
H_2S	Servomex	SERVOTOUGH Laserexact	Laser	0 – 10 ppm	2
SO_2	ThermoFisher SCIENTIFIC	iQ Series 43	Pulsated UV fluorescence	0 – 1 ppm	0.5

Table 2-2. Results from sensor validation tests

Gas component	Calibration gas concentration	Measured value
CO_2	10 %	8.76 %
H_2	500 ppm	245 ppm
H_2S	5 ppm	4.6 ppm
SO_2	0.5 ppm	549 ppb

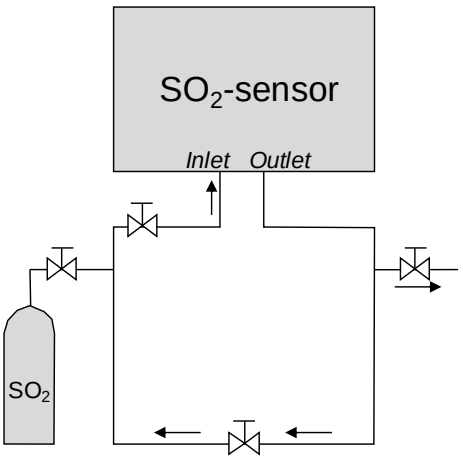

Figure 2-4**.** *Schematic flow scheme for validation of SO_2-sensor.*

2.2 Bentonite

The used bentonite comes from Milos and was provided by Imerys in Greece. The material (designated E8789) was processed in Germany. The characteristic of the delivered material, which was based on data from the supplier, is shown in Table 2-3. The material was also analysed within a characterization program at SKB (AP RD LERMTRL-20-014). This showed that the material exhibits a Tot/S content of approximately 0.9 % out of which approximately 1/3 is found as sulphide. In addition, the content of inorganic carbon was found to be about 3.5 % (as CO_2).

Table 2-3. Material specification of used bentonite provided by Imerys

Particle size	0.5 - 5.0 mm
Water content	13%
Montmorillonite content	65-75 %
Sulphur	~0.8%
Semi-activated	~30% Ca: 70% Na

2.3 Test matrix

Ten tests have been performed within this test program since the beginning, and a compilation of all tests with installed bentonite bulk mass, water content, operation temperature and test period are given in Table 2-4. The one test performed in the test container with copper heater was denoted PK_1. The remaining nine tests performed in the glass container in the heating cabinet were denoted GV_1 to GV_9. One goal of the GV tests was to investigate the influence of temperature and bentonite water content on the evolution of gas composition in general and the consumption of O_2 in particular. Whereas an analysis of the influence of the temperature has been achieved (see section 4.1), a corresponding analysis for the water content remains to be done. The results from the first two GV tests are not included in this report due to the extensive intrusion of air observed in these tests (see next section).

Table 2-4. Bentonite mass and test conditions applied in different tests

Test	Bulk mass (kg)	Water content (%)	Temperature (°C)	Test period	Remarks
PK_1	63.29	13.3	90*	210423-210618	-
GV_1	18.43	12.4	70	210224-210423	Not included here
GV_2	20.63	18.5	70	210423-210601	Not included here
GV_3	20.80	16.9	70	210601-210618	-
GV_4	20.98	16.7	70	210831-210928	-
GV_5	20.45	16.8	55	210929-211110	-
GV_6	21.09	15.9	55	211110-211216	-
GV_7	18.68	13.4	70	220120-220301	-
GV_8	19.94	14.7	70	220302-220405	-
GV_9	20.99	15.7	40	220405-220609	-

* Heater temperature

2.4 Development and challenges

Two major challenges have been encountered during the course of the work with this test programme.

The H_2-sensor

The expansion of the measuring range of the H_2-sensor was more complicated than initially thought, and this meant that this sensor had to be re-build by the manufacturer, and could therefore not be used during the first four tests (PK_1 and GV_1 through GV_3). After this modification, it was also noticed that the sensor had a recommended flow rate (0.3-0.4 L/min) which exceeded the

flow rate provided by the gas analysis system to the H_2-sensor (0.1 L/min), and results obtained from this are therefore thought to be underestimated (Table 2-2).

Leakages

During the first tests performed with the desiccator (GV_1 to GV_3) it was found that these were significantly affected by air intrusion, especially during measurements. The cooling of the extracted gas during such events could possibly lead to a gas pressure reduction, which in turn would lead to an inflow of air into the container. As a countermeasure, a gas pressure equilibration component (i.e. a balloon) was installed on the incoming tube to the glass container in May 2021. With this, it should be possible to contain the expansion of the gas caused by the initial heating of the test equipment, and also to have a surplus of gas volume which can be tapped during the measurements. A more significant improvement regarding the tightness was achieved by applying vacuum grease to the flanges in all such tests from the GV_4 tests and onward. However, also after this modification some minor, albeit significant, air intrusion was noticeable. A leakage search was therefore performed on October 29th 2021 (i.e. during the GV_5 test) with a Nordtec Testo 316-2 instrument, and by supplying a calibration gas with 500 ppm H_2 (see below) to the system. Two leaks were found during this search: i) a broken plastic T-coupling inside the O_2-sensor, which was replaced; and ii) the attachment/inlet to the H_2-sensor. The modification of the O_2-sensor seems to have been affected the calibration of this sensor, since O_2-depleted conditions have yielded results as low as -2 %. All O_2-results from test GV_6 and onwards have therefore been shifted +2%. The leakage point at the H_2-sensor has been remediated through grease application. However, it has been found to be difficult to seal this point completely.

3 Results

3.1 Gas evolutions in tests in glass container

Measured gas evolutions for four tests performed at 70 °C (GV_3, GV_4, GV_7 and GV_8) are shown in ***Figure*** 3-1. The water content of the bentonite installed in GV_3 and GV_4 was 2-3 %-units higher than in GV_7 and GV_8 (see Table 2-3). The first of these tests (GV_3) was affected by air intrusion after the first week, and to some minor extent also the other three tests were affected. Some general trends from these test results can nevertheless be identified:

- In GV_3, the O_2 decreased from typical air concentration to 10 % during the first 3 days. In the other three tests the O_2 decreased to low levels, close to 0%, in approximately 7 to 10 days.
- In GV_4, GV_7 and GV_8, the CO_2 and H_2S increased during the first two weeks to fairly stable levels, with 11-13 % CO_2 and 11-14 ppm (H_2S), respectively. The last CO_2 and H_2S concentrations in the GV_3 were also found in these intervals.
- The SO_2 increased during the first two weeks to approximately 900-1200 ppb. In GV_4 and GV_8, this concentration was reduced to approximately half that level during the subsequent two weeks.
- The H_2 increased during the first week to 200 - 700 ppm, after which it was reduced with a factor of 3 or more during the subsequent three weeks. It can be noted that maximum value in the GV_4 test was more than twice as high as in the GV_7 and GV_8 tests. This shift was probably caused by an attempt to calibrate the H_2-sensor during the GV_5 test.

Measured gas evolutions from two tests performed at 55 °C (GV_5 and GV_6), and one test performed at 40 °C (GV_9), are shown in ***Figure*** 3-2. The first of these (GV_5) was affected by air intrusion and it was during this test that a leakage search was conducted and the broken T-

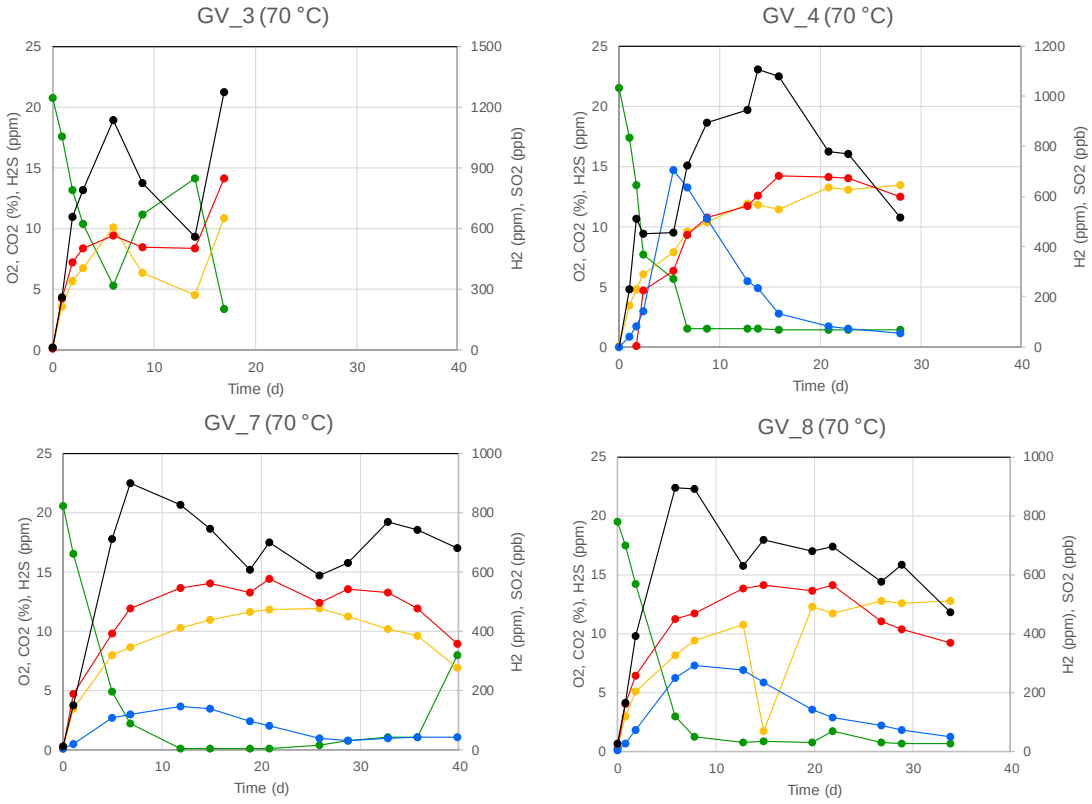

Figure 3-1. *Test results for four tests in glass desiccator at 70 °C. O_2 (green), CO_2 (orange), H_2S (red), H_2 (blue) and SO_2 (black). The O_2 data has been shifted +2% for test GV_7 and GV_8.*

coupling inside the O_2-sensor was replaced. The significant air intrusion observed after five weeks was caused by the human factor and an open valve.

The results from the second test performed at 55 °C (GV_6) indicate that the test system was more gas tight than in the previous test. The decreasing O_2 trend during the first two weeks indicates that the rate of oxygen consumption was quite constant with approximately 1 % unit per day. After this the O_2 concentration displayed a more asymptotic decreasing trend and never fell below 3 % during the measurements. In parallel to this, the concentration of the other gas components increases to fairly constant levels; CO_2: 4 %, H_2S: 5 ppm, H_2: 200 ppm, and SO_2: 600 ppb.

The results from the test performed at 40 °C (GV_9) also indicate that the test system was fairly gas tight. In this case the overall rate of O_2 consumption was approximately 0.05 % per day. However, the oxygen reduction between some consecutive measurements was almost twice as high, and this indicates that a minor air intrusion did occur during each measurement. In this test, the concentration of CO_2 increased to 0.8 %, H_2 to 60 ppm, SO_2 to 130 ppb, whereas H_2S was below 1 ppm.

Apart from the measurements performed with the gas analysis system, the acquirement of the leakage detector mentioned above has also enabled qualitative measurements of CH_4 by inserting the sensor head of the instrument into the glass container at the time of dismantling. Such measurements have been performed on several tests from the GV_4 test and onward, and indicate a significant concentration (>1%) of CH_4.

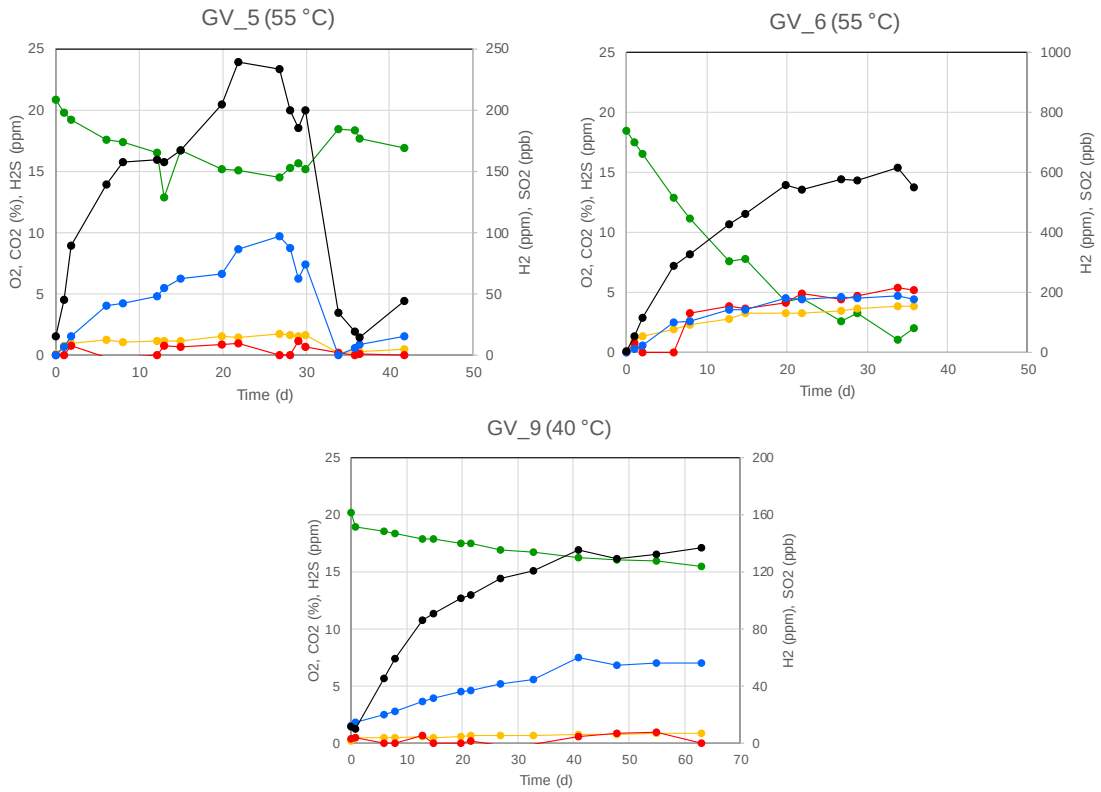

Figure 3-2. *Test results for tests in glass desiccator at 55 and 40 °C, respectively. O_2 (green), CO_2 (orange), H_2S (red), H_2 (blue) and SO_2 (black). The O_2 data has been shifted +2 % for test GV_6 and GV_9.*

3.2 PK_1 test in container with copper heater

Evolutions of measured gas components, temperature and relative humidity in the PK_1 test are shown in ***Figure*** 3-3. The temperatures measured at different heights and at 80 mm distance from the container wall (***Figure 2-1***) were generally found within the interval 30 to 40 °C. Similarly, the relative humidity values measured at 60 mm from the wall, were generally found within the interval 70 to 80 %. The rate of O_2 consumption was quite modest and the O_2 concentration never fell below 17 % during the eight-week test period. This appears to some extend to be caused by air intrusion, e.g. after the first week when the O_2 concentration increased, and the SO_2 and CO_2 concentrations decreased from 140 to 20 ppb, and from 1.1 to 0.5 %, respectively. However, it can be noted that the overall temperature level in the bentonite around the heater was quite low (***Figure*** 3-3, lower left), and the conditions in this test therefore appears to resemble those in the GV_9 test (with 40 °C) most closely among the tests performed in glass container. The test system appears to have been more gas tight during the last few measurements of the test, since the O_2 concentrations again decreased while the SO_2 and CO_2 concentrations increased. Finally, the water content distribution was measured at the end of the test (***Figure*** 3-3, lower right), and this showed that a noticeable moisture redistribution had occurred due to the thermal gradients in the bentonite.

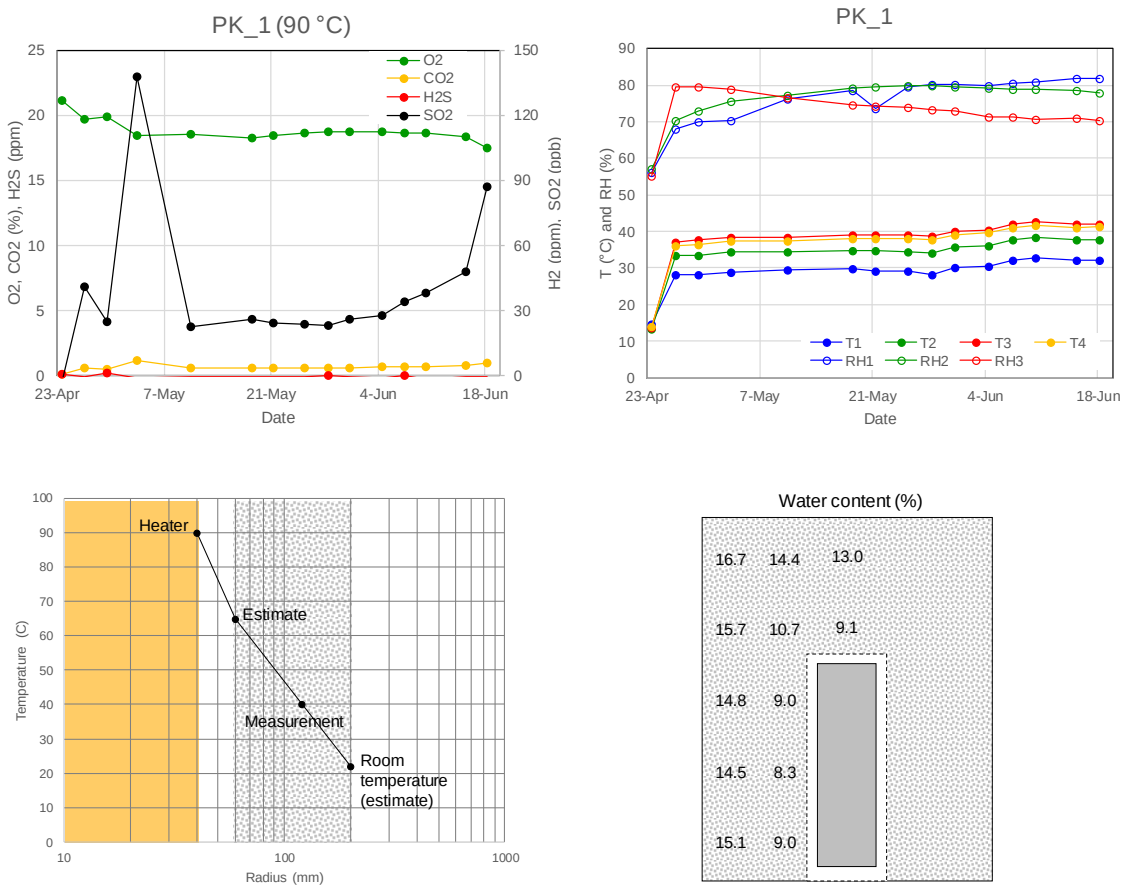

Figure 3-3. *Test results for test PK_1 in container with copper heater. Evolution of gas components (upper left) and temperature and relative humidity; sensor positions according to Figure 2-1 (upper right). An evaluation of the temperature profile at heater mid-height (lower left). Water content distribution at the end of the test (lower right).*

4 Evaluations

4.1 Temperature dependence of the rate of O_2 consumption

The temperature dependence of the rate of O_2 consumption was evaluated from data measured during the initial phase of five of the tests performed in glass container. Two of these were performed at 70 °C (GV_3 and GV_4); two at 50°C (GV_5 and GV_6); and one at 40°C (GV_9). Two additional tests performed at 70°C (GV_7 and GV_8) could also have been addressed, but the water content in these tests were slightly lower than in the other tests (Table 2-4) and therefore not included in this evaluation. Still, for comparisons, the data from these two tests are included in ***Figure*** 4-1 below.

The oxygen consumption rates used in the evaluation was simply defined as the concentration decrease per unit time (i.e. %/day). This was deemed to be sufficiently detailed, since the bulk mass and the water content in the different tests were quite similar. The evolution of O_2 consumption was simply evaluated as the difference between the first and the subsequent measurements for each test (between the second and subsequent measurements in GV_9 due to the marked initial concentration drop in this test). From these evolutions, the following consumption rates were evaluated: 4.5, 1 and 0.1 %/day for 70, 55 and 40 °C, respectively (***Figure*** 4-1, upper row). By plotting the logarithm of these consumption rates versus the inverse of the absolute temperature (***Figure*** 4-1, lower left), an activation energy of approximately 0.11 MJ/mol can be evaluated. A comparison of an exponential temperature dependence with this activation energy and the evaluated consumptions rates is shown in ***Figure*** 4-1 (lower right).

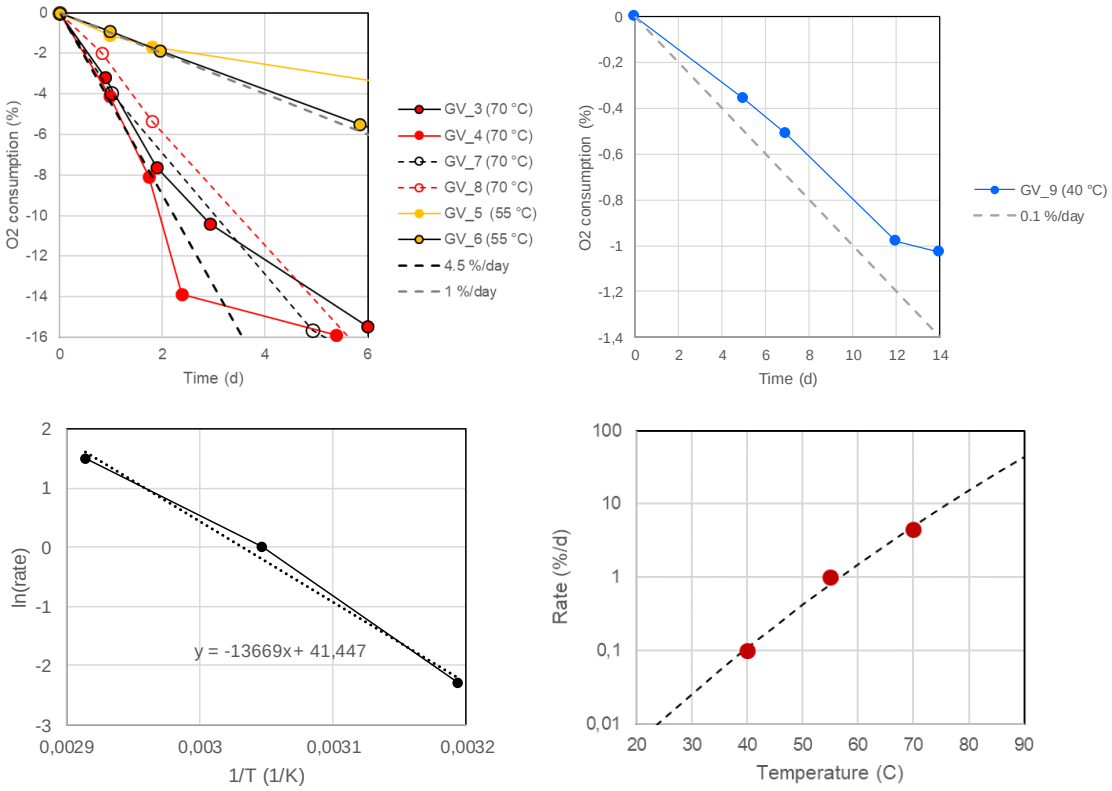

Figure 4-1. *Evaluation of temperature dependence of the rate of oxygen consumption in tests in glass containers. Evolution of O2 consumption in five tests (upper row). Arrhenius plot (lower left) and exponential temperature dependence together with measure consumptions rates (lower left).*

4.2 Tentative conceptual model

Since there are no metals in the glass container, and since a clear generation of SO_2 can be measured, it appears to be quite evident that oxygen is consumed through pyrite oxidation. This process probably occurs in the presence in water, since the O_2 concentration reduction exceeds by far the concentration of SO_2. The formation of CO_2 indicates the dissolution of calcite. This process requires the formation of H^+, which in turn also indicates pyrite oxidation in the presence of water. Pyrite oxidation does not lead to the formation of H_2S, if the sulphur is oxidized. Pyrite dissolution could therefore be the source of H_2S (see King 2013). The formation of methane, as qualitatively measured with the leakage detector, can tentatively originate from either degradation of organic material, or through hydrogenotrophic methanogenesis.

A simple mass balance calculation shows that the amounts of pyrite and calcite in the bentonite are sufficient to explain the complete consumption of all O_2 and the generation of all observed CO_2. Installed amounts of bentonite, water and air in one the glass container tests are shown in Table *4-1*. The initial amounts of O_2 in the gas phase and sulphide-S in the bentonite can then be calculated as:

- $n_{O2}=C_{O2} \cdot V_G \cdot / V_m = 21\ \% \cdot 12.7$ litre / 24 litre/mol = 0.11 mol
- $n_S = x_S \cdot m_d / M_S = 0.003$ kg/kg $\cdot 17.8$ kg / 0.032 kg/mol= 1.7 mol

By the same token, the final amount of CO_2 in the gas phase and the initial amount of inorganic carbon in the bentonite can be calculated as:

- $n_{CO2,gas} = C_{CO2} \cdot V_G \cdot / V_m = 10\ \% \cdot 12.7$ litre / 24 litre/mol = 0.05 mol
- $n_{CO2,bentonite} = x_{CO2} \cdot m_d / M_{CO2} = 0.035$ kg/kg $\cdot 17.8$ kg / 0.044 kg/mol= 14 mol

This clearly shows that the amount of sulphide-S in the bentonite is sufficient to consume all the O_2 in the gas phase, and that the initial amount of inorganic carbon far exceeds the amount of CO_2 in the gas phase at the end of the test.

The unsaturated bentonite can generally be considered to be composed of three phases: solid, liquid and gas phase. Whereas the gas phase can be assumed to be fairly homogenous, the other two are probably quite heterogenous. Due to the hydroscopic properties of the montmorillonite, it can be assumed that the dominant part of the liquid phase is absorbed in the montmorillonite, and that only a small fraction of this phase is attached with the accessory minerals (***Figure 4-2***). This means that the water volume where the chemical reactions take place may be much smaller than the gas volume.

Table 4-1. Specification of material and phases in glass container setup (test GV_3)

Bentonite mass	20.8 kg
Volume (lower part)	17.4 litre
Water content	16.9 %
Density (bulk)	1195 kg/m3
Density (dry)	1023 kg/m3
Density (solid)	2750 kg/m3*
Void ratio (e)	1.69 (-)
Porosity (n)	0.63 (-)
Degree of saturation (S)	0.28 (-)
n*(1-S)	0.46 (-)
Gas volume (lower part)	7.9 litre
Gas volume (upper part)	4.8 litre
Gas volume (total)	12.7 litre
Water volume	3.0 litre

* Adopted from Karnland et al. (2006)

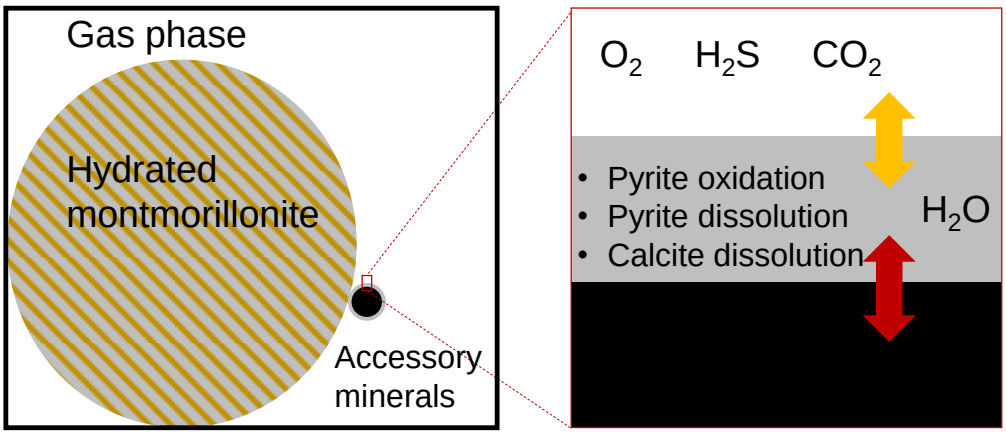

***Figure 4-2**. Tentative description of the site of the reactions of interest.*

5 Future work

This status report has presented results obtained within the framework of the activity plan AP RD LERMTRL-20-018 during the first 18 months of measurements. A number of measures and modifications could or should be addressed during the continuation of this work.

- *Service and calibration of sensors.* The CO_2-sensor should be sent to the manufacturer (Vaisala), whereas all other sensors should be subject for maintenance by the supplier (OmniProcess).
- *Modified flow rate through H_2 sensor*. The designed flow rate through the H_2 sensor (0.1 L/min) is currently not optimal for the sensor (0.3-0.4 L/min). This could possibly be rectified by installation of a new valve. It would also be advantageous if the attachment/inlet to the H_2-sensor could be sealed completely.
- *New sensors.* Tests with the leak sensor at the dismantling of some of the tests indicates that there was a noticeable formation of CH_4 in these tests. In order to obtain more detailed and reliable data on such a formation, it is proposed that that the gas analysis system is complemented with a CH_4 sensor.
- *Other analyses.* It would be beneficial if the interpretation of the measured evolution of gases could be supported by other types of analyses, e.g. pH which tentatively can be measured with a universal pH indicator after dispersion of the material in a solid:liquid ratio of 1:3 (Olsson et al. 2013).
- *Smaller glass container*. The amount of bentonite required for each test could be reduced by replacing the current glass container with a smaller one.
- *Influence of bentonite water content.* Tests with significantly higher, and perhaps lower, water content should be performed in order to investigate the influence of this parameter.
- *Other materials.* It would be interesting to tests the methodology on other material. Not only on other bentonites such at MX-80, but also on “pure” pyrite. It would also be advantageous to perform at least one control test with an empty air-filled glass container.
- *Modification of equipment test container with copper heater*. The PK_1 test demonstrated that the temperature in the bentonite in this test was relatively low. The design of this equipment should therefore be modified, first and foremost by installation of thermal insulation on the outer surfaces of the test container. Secondly, if possible, the diameter of the perforated cage around the heater should be reduced.

References

SKB's (Svensk Kärnbränslehantering AB) publications can be found at www.skb.com/publications.

Birgersson M, Goudarzi R, 2018. Investigations of gas evolution in an unsaturated KBS-3 repository. SKB TR-18-11, Svensk Kärnbränslehantering AB.

Karnland O, Olsson S, Nilsson U, 2006. Mineralogy and sealing properties of various bentonites and smectite-rich clay materials. SKB TR-06-30, Svensk Kärnbränslehantering AB.

King F, 2013. A review of the properties of pyrite and the implications for corrosion of the copper canister. SKB TR-13-19, Svensk Kärnbränslehantering AB.

Olsson S, Jensen V, Johannesson L-E, Hansen E, Karnland O, Kumpulainen S, Svensson D, Hansen S, Lindén J, 2013. Prototype Repository. Hydromechanical, chemical and mineralogical characterization of the buffer and backfill material from the outer section of the Prototype Repository. SKB TR-13-21, Svensk Kärnbränslehantering AB.

Åkesson M, Svensson D, Laitinen H, 2020. Gas phase composition during the unsaturated period. Initial tests. SKB P-20-23, Svensk Kärnbränslehantering AB.